Agricultural and Forest Meteorology 249 (2018) 286–296

Contents lists available at ScienceDirect

Agricultural and Forest Meteorology

journal homepage: www.elsevier.com/locate/agrformet

Research Paper

Dual effect of precipitation redistribution on net ecosystem CO_2 exchange of a coastal wetland in the Yellow River Delta

Xiaojing Chu[a,b], Guangxuan Han[a,*], Qinghui Xing[a,b], Jianyang Xia[c], Baoyu Sun[a,b], Junbao Yu[d,*], Dejun Li[e]

[a] Key Laboratory of Coastal Environmental Processes and Ecological Remediation, Yantai Institute of Coastal Zone Research, Chinese Academy of Sciences, Yantai 264003, China
[b] University of Chinese Academy of Sciences, Beijing 100049, China
[c] School of Ecological and Environmental Sciences, East China Normal University, Shanghai 200241, China
[d] School of Resources and Environmental Engineering, Ludong University, Yantai 264025, China
[e] Institute of Subtropical Agriculture, Chinese Academy of Sciences, Changsha 410215, China

ARTICLE INFO

Keywords:
Precipitation redistribution
Net ecosystem CO_2 exchange
Salt stress
Waterlogged stress
Coastal wetland

ABSTRACT

Hydrological regime is crucial in determining the carbon dioxide (CO_2) exchange between the atmosphere and wetlands. Seasonal redistribution of precipitation is one featured hydrological regime shift, but its impacts on ecosystem CO_2 exchange in coastal wetlands remain unclear. Here, based on the eddy-covariance technique, we examined how the net ecosystem CO_2 exchange (NEE) in a coastal wetland of Yellow River Delta in China differed between two years (2012 and 2013) with contrasting seasonal distribution of precipitation. The ecosystem absorbed more CO_2 during the growing stage in 2013 (-268.5 g C m^{-2}) than 2012 (-174.7 g C m^{-2}). This difference resulted from higher NEE in the fast and middle growth stages with different reasons. In the fast growth stage, the higher mean daily NEE occurred due to more precipitation coupled with lower salt stress in 2013 (-6.3 g CO_2 m^{-2} day^{-1}) compared to that in 2012 (-2.2 g CO_2 m^{-2} day^{-1}). During the middle growth stage, the mean daily NEE in 2013 (-4.2 g CO_2 m^{-2} day^{-1}) was significantly higher than that in 2012 (-1.1 g CO_2 m^{-2} day^{-1}) because the ecosystem in 2012 suffered more waterlogged stress. This dual effect of precipitation distribution on vegetation photosynthesis was also observed in a field manipulation experiment at the same site. Our results indicated that the redistribution of precipitation among seasons would play a critical role in regulating ecosystem CO_2 exchange in the coastal wetland. More research on the associated changes between dynamics of soil hydrology and salinity could promote the accuracy of the carbon-budget estimates in coastal wetlands.

1. Introduction

Global climate models project that changes in the frequency and amplitude of extreme meteorological events can result in seasonal redistribution of the precipitation, characterized by fewer and larger precipitation events (Allen and Ingram, 2002; Semenov and Bengtsson, 2002; IPCC, 2007; Knapp et al., 2008). Such changes are expected to continue throughout the current century (Easterling et al., 2000; Min et al., 2011). Drought and flooding caused by the precipitation redistribution could impact soil moisture conditions and profoundly alter the structure, functioning and processes of an ecosystem, including the carbon (C) balance (Hussain et al., 2011; Biederman et al., 2016; Jia et al., 2016). The impacts of drought or flooding caused by the precipitation distribution on the CO_2 exchange of an ecosystem have been studied for a range of ecosystems (Nagy et al., 2007; Noormets et al., 2008; Wu et al., 2011; Scott et al., 2015; Liu et al., 2016), including grassland (Bowling et al., 2015; Sloat et al., 2015), shrubland (Ross et al., 2012; Jia et al., 2016), forest (Bonal et al., 2008; Doughty et al., 2015), mire (Aurela et al., 2007; Leppälä et al., 2011; Lund et al., 2012).

Precipitation may directly or indirectly affect the uptake of CO_2 during photosynthesis and the emissions of CO_2 via respiration as well as decomposition in several different aspects, which subsequently affect NEE (Leppälä et al., 2011; Lund et al., 2012; Doughty et al., 2013; Doughty et al., 2015). On the one hand, the paucity of precipitation can result in little plant growth (Rajan et al., 2013). Compared with the full

* Corresponding authors at: Key Laboratory of Coastal Zone Environmental Processes and Ecological Remediation, Yantai Institute of Coastal Zone Research, Chinese Academy of Sciences, 264003 Yantai, Shandong, China.
E-mail address: gxhan@yic.ac.cn (G. Han).

http://dx.doi.org/10.1016/j.agrformet.2017.11.002
Received 8 August 2017; Received in revised form 2 November 2017; Accepted 2 November 2017
Available online 07 November 2017
0168-1923/

canopy stage, vegetation is most sensitive to droughts during the leaf out and canopy development stages, when the plant's metabolic activity, such as photosynthesis and respiration, can be suppressed by drought (Kwon et al., 2008; Lund et al., 2012; Rajan et al., 2013). On the other hand, when precipitation is excessive and soils become waterlogged, the diffusion of oxygen into soil will be limited. Subsequently, heterotrophic respiration is likely suppressed due to lowered microbial activity and decomposition rates of organic matter (Heinsch et al., 2004). In addition, flooding conditions affect the sensitivity of CO_2 exchange to variations in light and temperature, which in turn influence the uptake of CO_2 in ecosystems (Chivers et al., 2010; Jimenez et al., 2012).

Coastal wetlands, the interfaces between terrestrial and ocean ecosystems, play an important role in the global C cycle by acting as natural carbon (C) sinks (Crooks et al., 2011). Coastal wetlands accumulate organic matter because of their relatively high net primary productivity coupled with a relatively low rate of decomposition of accumulated organic matter (Drake et al., 2015). Most area of a coastal wetland lies beyond the reach of the tides, and its hydrologic regimes is dominated by the interaction of precipitation and a shallow, saline water table in the vertical direction (Zhang et al., 2011; Han et al., 2015). During dry seasons, usually with a limited precipitation supply, water-soluble salts from the groundwater are transported upward to the root zone and soil surface through capillary rise. Exposed to increasing salinity levels, the coastal wetland behaves more as a dryland ecosystem than a wetland (Zhang et al., 2011; Yao and Yang, 2013). During the rainy season, though precipitation can leach salts from the plant root zone, episodic flooding is often observed (Han et al., 2015). The salt accumulation and leaching induced by the seasonal precipitation distribution have a profound impact on the carbon biogeochemical cycle and carbon balance by regulating the salinity and waterlogged stress of plants (Heinsch et al., 2004). Therefore, understanding the responses of NEE to the precipitation distribution is essential not only for predictive modeling of potential short- and long-term changes of carbon storage but also for predicting the possible impacts of climate change. However, the mechanisms underlying the impacts of the precipitation distribution on the ecosystem CO_2 exchange in a coastal wetland have so far received little attention.

The net ecosystem CO_2 exchange (NEE) between an ecosystem and the atmosphere relies on the balance between CO_2 uptake through plant photosynthesis and ecosystem respiration through plant and soil respiration (Iii et al., 2006). The micrometeorological eddy covariance (EC) technique has been widely used to quantify NEE between the atmosphere and the vegetation surface in various wetlands because it can provide continuous, long-term flux information integrated at the ecosystem scale (Aubinet et al., 1999; Baldocchi et al., 2001; Baldocchi, 2008; Ross et al., 2012). Using eddy covariance, our study was conducted in a coastal wetland of the Yellow River Delta, where the hydrologic regimes are dominated by the interaction of precipitation and a shallow, saline water table in the vertical direction. Fortuitously, the amounts of rainfall in 2012 and 2013 were similar, but the precipitation distributions during the different growing stages were significantly different. This offers a special opportunity to investigate the impact of the precipitation distribution on CO_2 exchange in a coastal wetland. The main objectives of this study were to assess the effect of the precipitation distribution on the magnitude of NEE and its light and temperature response in a coastal wetland.

2. Materials and methods

2.1. Site description

The study was conducted in the Yellow River Delta Ecological Research Station of Coastal Wetland (37°45′50″N, 118°59′24″E), which belongs to Yantai Institute of Coastal Zone Research, Chinese Academy of Sciences. The flux tower is located approximately 3 km south of the Yellow River channel and approximately 20 km southwest of the mouth of the Yellow River. The experimental site has a warm temperate and continental monsoon climate with distinctive seasons and distributions of rain and heat. The annual average temperature is 12.9 °C, and the average annual precipitation is 550–640 mm, with nearly 74% of the precipitation falling between June and September. The prevailing wind direction in the growing season is from the northeast to the southeast (Han et al., 2013). The soil type in the Yellow River Delta gradually varies from fluvo-aquicto saline soil, and the soil texture is mainly sandy clay loam. Due to the flat terrain and high groundwater table, the entire area is covered mainly by wet and saline soil (Nie et al., 2009). In most of the areas, the groundwater levels range from 1 to 3 m with high water salinity (5–30 g L^{-1}) (Min et al., 2009; Fan et al., 2011), which is affected by fresh water and salt water (Guan et al., 2001; Fan et al., 2011; Zhang et al., 2011; Zhong et al., 2013).

The vegetation is relatively homogeneous and strongly dominated by common reed (*Phragmites australis*), with other associated species including *Tamarix chinensis*, *Tripolium vulgare*, *Suaeda salsa* and *Imperata cylindrical*. The growth stages of the natural growth cycle (DOY 97–311) were divided from the phenophase (2012 and 2013) and pentad temperature (daily mean air temperature for 5 consecutive days of 1961–2011). During the fast growth stage (DOY 97–199), defined as the time between the first pentad temperature for 10 °C and the first peak aboveground biomass, the aboveground biomass increased rapidly during this stage. During the middle growth stage (DOY 200–260), defined as the stage from the first peak aboveground biomass to the second peak aboveground biomass, vegetation posted slower growth for booting and heading during this stage. During the terminal growth stage (DOY 261–311), representing the time from the second peak aboveground biomass to the first pentad temperature for 10 °C, the community senesced during this stage.

2.2. Eddy covariance and meteorological measurements

Eddy covariance and microclimate measurements were conducted at the site during 2012 and 2013. Ecosystem CO_2 fluxes were measured using an EC system mounted 3.0 m above the soil surface. The densities of CO_2 and H_2O were measured by an open-path infrared gas analyzer (IRGA, LI-7500, LI-COR Inc., USA), and the three wind components and the speed of sound were measured with a three-axis sonic anemometer (CSAT-3, Campbell Scientific Inc., USA). Raw data outputs from the

IRGA and sonic anemometer were collected at 10 Hz and recorded by a data logger (CR1000, Campbell Scientific Inc., USA) at 30 min intervals. The IRGA was calibrated once or twice every year in the laboratory using pure nitrogen gas, CO_2 calibration gas, and a dew point generator (LI-610, Li-COR Inc., USA). As the uniform fetch was at least 300 m in all directions, the majority of fluxes came from the target area.

Meteorological parameters were measured with an array of sensors. Net radiation was measured at a height of 3.0 m with a four-component net radiometer (CNR4, Kipp & Zonen Netherlands Inc., Bohemia, NY, USA). Photosynthetic active radiation (PAR) was measured above the canopy at a height of 3.0 m using quantum sensors (LI-190SB, Li-Cor Inc., USA). Air temperature and relative humidity were measured at the height of 2.5 m (HMP45C, Vaisala, Helsinki, Finland). Other environmental variables measured included wind speed and direction (034B, Met One Inc., USA), precipitation (TE525 tipping bucket gauge, Texas Electronics, Texas, USA), soil temperature at 5, 10, 30, and 50 cm depths below the surface (109SS, Campbell Scientific Inc., USA), and SWC at 5, 10, 20, 40, 60, 80, and 100 cm depths below the surface (EnviroSMART SDI-12, Sentek Pty Ltd., Australia). More details about the meteorological measurements are presentated elsewhere (Han et al., 2015). All meteorological data were measured every 15 s and then averaged half hourly by a data logger (CR1000, Campbell Scientific Inc., USA).

2.3. Flux data processing and quality control

Mean flux data on a half-hour time scale were calculated using the EdiRe software (University of Edinburg, Scotland). The 10-Hz raw eddy covariance data were applied to screen out anomalous values, and the filtered data were used to calculate half-hourly CO_2 fluxes. The Webb-Pearman-Leuning (WPL) correction and three-dimensional coordinate rotation (3-D rotation) were used to adjust the half-hourly CO_2 flux data (Webb et al., 1980; Polsenaere et al., 2012). Then, quality tests on stationarity and turbulence development conditions of the half-hourly CO_2 flux data were performed using the software, allocating quality signals to every data point (Kaimal and Finnigan, 1994).

Subsequently, the half-hourly CO_2 flux data outputted by EdiRe software were further filtered according to a series of standards before they were used for later analysis. The excluded data mainly included the following:

(1) The half-hour flux data before and after precipitation
(2) The CO_2 flux data whose absolute value (|NEE|) exceeded 60 μ mol CO_2 m^{-2} s^{-1} (Zhou et al., 2009; Han et al., 2013)
(3) The CO_2 flux data when the air turbulence was weak, especially when friction velocity (u*) < 0.15 m s^{-1} (Han et al., 2015).
(4) The CO_2 flux data that were smaller than zero when Rn < 10 W m^{-2}

Following these screenings and tests, roughly 42% of the data obtained from the EC system was rejected during the whole study period.

2.4. Flux gap filling and component partitioning of the CO_2 flux

We used the following procedure to fill missing and bad data to provide estimates for the balance of NEE. Small gaps (less than 2 h) were filled by linear interpolation. Large gaps (more than 2 h) were filled based on separate empirical models for daytime and nighttime data. When PAR was > 10 μmol m^{-2} s^{-1}, the missing daytime NEE data during the growing season were gap filled using the Michaelis–Menten model (Ruimy et al., 1995; Falge et al., 2001),

$$NEE = -\frac{A_{max}\,\alpha PAR}{A_{max} + \alpha PAR} + R_{eco,\,day} \quad (1)$$

where the coefficient α is the apparent quantum yield (mg CO_2 μmol^{-1} photon), A_{max} is the light-saturated net CO_2 exchange (mg CO_2 m^{-2} s^{-1}), and $R_{eco,day}$ is the daytime ecosystem respiration (mg CO_2 m^{-2} s^{-1}) and PAR is the photosynthetically active radiation (μmol m^{-2} s^{-1}).

When PAR was < 10 μmol m^{-2} s^{-1}, the missing nighttime NEE data were filled with the exponential relationship between R_{eco} and the soil temperature at 5 cm function (Lloyd and Taylor, 1994):

$$R_{eco,\,night} = a\exp(bT) \quad (2)$$

where $R_{eco,night}$ is the nighttime NEE, T is the air or soil temperature (°C), and a and b are two empirical coefficients.

Q_{10} can be estimated as follows:

$$Q_{10} = \exp(10b) \quad (3)$$

Daily R_{eco} is the sum of daytime ecosystem respiration ($R_{eco,day}$) and the nighttime ecosystem respiration ($R_{eco,night}$):

$$R_{eco} = R_{eco,day} + R_{eco,night} \quad (4)$$

Daily gross primary productivity (GPP) was calculated as follows:

$$GPP = R_{eco} - NEE \quad (5)$$

2.5. Precipitation manipulation experiment

To gain new insights into the underlying mechanism responsible for the effects of precipitation on ecosystem CO_2 exchange, a precipitation manipulation experiment was established in the same site, 300 m away from the EC tower. The experiment was completely randomized block designed in May 2015, consisting of twelve 3 × 4 m^2 plots, with 4 replicates each consisting of three levels of precipitation [ambient (CK), wet (+40%) and drought (−40%)]. Before the experiment, isolation belts (0.2 m deep, 0.3 m height and 0.5 m width) were built around each plot and lined with two layers of polyethylene sheeting to prevent the lateral movement of water and nutrients between individual plots and their surroundings.

The experiment infrastructure used passive removal and active distribution systems to manipulate precipitation. Above the −40% zone, a rainout shelter with 16 of 10-cm-wide corrugated clear polycarbonate slats distributed evenly removed 40% of incoming precipitation. During the growing seasons, this water drained into storage tanks and was immediately transferred to the +40% zone via a sprinkler system, to achieve a 40% increase in each precipitation event. Treatments of CK and +40% lie under a similar structure and receive mild shading to match that of rainout shelters. In the experiment, SWC and soil salinity at 10 cm depth approximately were measured every 30 min using sensors of 5TE (Decagon, USA). Ground water level was recorded every two weeks during the middle growth stage. Pn (net photosynthetic rate) −PAR response curve was measured on fully expanded, exposed current-year leaves under controlled optimal conditions using an open-mode portable photosynthesis system (LI-6400, Li-Cor, USA) every two weeks from May to October. Response of Pn to PAR were measured at 0, 50, 80, 100, 200, 400, 600, 800, 1000, 1200, 1500, 1800, and 2000 μmol m^{-2} s^{-1}.

2.6. Aboveground biomass

Aboveground biomass for the coastal wetland was measured by harvesting the vegetation approximately twice a month during the growing season (from May to October) from 2012 to 2013. Harvesting was performed in five replicated sampling plots (0.5m × 0.5 m) located within a radius of 200 m around the EC system. Live plants were clipped at 1 cm above the ground level. Plant aboveground biomass was oven dried at 80 °C to a constent weight before weighing.

2.7. Statistical analysis

A paired samples *t*-test was used to test the significant differences in environmental factors (SWC, PAR and T_{air}) and the mean daily values of NEE during the fast, middle and terminal growth stages between two years. On the basis of half-hourly data, the light and temperature response to daytime NEE and nighttime NEE during the fast, middle and terminal growth stages were investigated using Eqs. (1) and (2), respectively, through which the parameters of both the nonlinear relationship were estimated during the fast, middle, terminal and the entire growing stages, respectively. On the basis of daily mean data, simple linear relationships were fitted between R_{eco} and GPP during the fast, middle, terminal and the entire growing stages, respectively. In the precipitation manipulation experiment, SWC, soil salinity and net photosynthetic rate were calculated as the mean of four replicates at random locations for each treatment. We used the repeated measure analysis of variance (ANOVA) to test the differences in SWC, soil salinity and net photosynthetic rate. All statistical analyses were performed using SPSS 11.5 (SPSS for Windows, Version 11.5, Chicago, IL, USA).

3. Results

3.1. Comparison of precipitation distribution and environmental factors

The frequency distributions of the precipitation during each growing stages were very similar in shape but varied substantially in amplitude of the study region from 1961 to 2011 (Fig. 1). The total

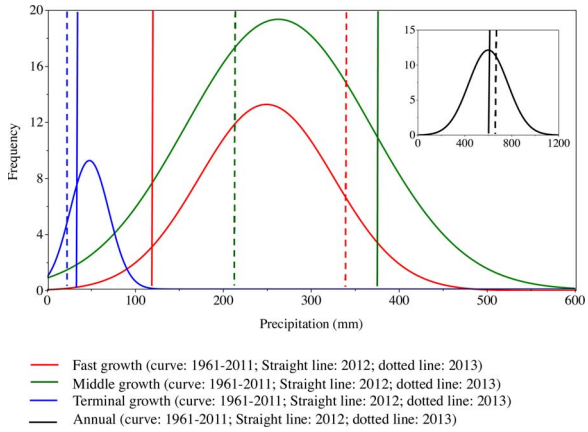

Fig. 1. The frequency distributions of the precipitation during each growing periods (red solid curve represents the fast growth period, green solid curve represents the middle growth period, blue solid curve represents the terminal growth period, dark solid curve represents the entire growing season) of the study region from 1961 to 2011. The vertical solid lines and dotted lines represent precipitation of 2012 and 2013 during each growing periods (red lines represent the fast growth period, green lines represent the middle growth period, blue lines represent the terminal growth period, dark lines represent the entire growing season), respectively. (For interpretation of the references to colour in this figure legend, the reader is referred to the web version of this article.)

rainfall amounts in 2012 and 2013 were similar (615.2 and 634.0 mm, respectively) (Fig. 1). Most precipitation distribution was concentrated in the growing season (87% in 2012 and 91% in 2013), with roughly 72% falling in the middle growth stage of 2012, and 59% during the fast growth stage in 2013 (Fig. 1, Table 1).

The precipitation during the 2013 fast growth stage was 341.1 mm, which was above (149%) the long-term mean (1961–2011, 229.3 mm) for the same stage (Figs. 1, 2 a and Table 1). In contrast, the precipitation during the fast growth stage in 2012 was only 123.4 mm (36% of the amount in 2013), which was below (54%) the long-term mean. The precipitation distribution variation was reflected particularly in the significant difference in SWC (Fig. 2b and Table 1). The exceptionally dry fast growth stage in 2012 was coupled with a lower average SWC than 2013 ($P < 0.01$). The precipitation during middle growth stage in 2012 was 384.2 mm (174% of the long-term mean), distinctly higher than that in 2013 (215.0 mm), which was coupled with a higher average SWC than 2013 (Fig. 2b and Table 1, $P < 0.05$). The SWC values during the terminal growth stages were similar between the two years due to the lower precipitation compared with the long-term mean. The PAR values recorded during the middle and terminal growth stages were similar in both years, however, the PAR values recorded during the fast growth stage in 2012 were higher than those recorded in 2013 (Table 1, $P < 0.05$). Significant differences between the 2 yr were also observed in air temperature (T_{air}) during the fast growth stage, but T_{air} values were similar during the middle and terminal growth stages (Table 1).

The value of aboveground biomass increased rapidly during fast growth period, it posted slower growth during middle growth period, followed by a gradual decline as the community senesced during the terminal growth period. Due to the earlier rainfall and more favorable weather conditions, the phonological development was faster in 2013 than in 2012 (Fig. 2c).

3.2. Seasonal variation in NEE during the different growth stages

The daily accumulated NEE of 2012 and 2013 showed distinct seasonal patterns, which indicated their responses to the combined effects of weather and vegetation growth. The average NEE of 2012 exhibited a smaller range of variation than that of 2013 (Fig. 2d). During the fast growing season, NEE was primarily triggered by precipitation. The daily NEE values increased more quickly (Fig. 2d) with earlier

Table 1
Seasonal average of precipitation (PPT), soil water content at 10 cm depth (SWC), photosynthetic active radiation (PAR), air temperature (T_{air}), and mean daily NEE during each growing atages of 2012 and 2013 in the coastal wetland.

Parameter	Fast Growth (DOY 97–199)				Middle Growth (DOY 200–260)				Terminal Growth (DOY 261–311)			
	1961–2011	2012	2013	*P*-value	1961–2011	2012	2013	*P*-value	1961–2011	2012	2013	*P*-value
PPT, mm	229.3	123.4	341.1	–	221.1	384.2	215.0	–	53.0	30.0	18.2	–
SWC, %	–	38.1	41.0	0.003	–	52.7	50.6	0.025	–	41.0	40.3	> 0.05
PAR, μmol m^{-2} s^{-1}	–	53.1	47.2	> 0.05	–	45.1	45.7	> 0.05	–	21.1	19.5	> 0.05
T_{air}, °C	20.9	20.9	19.5	> 0.05	25.3	25.7	25.9	> 0.05	16.3	16.6	16.4	> 0.05
NEE, g CO_2 m^{-2}day^{-1}	–	−2.2 ± 0.2	−6.3 ± 0.5	0.001	–	−1.1 ± 0.3	−4.2 ± 0.5	0.003	–	−1.1 ± 0.2	−1.5 ± 0.3	> 0.05

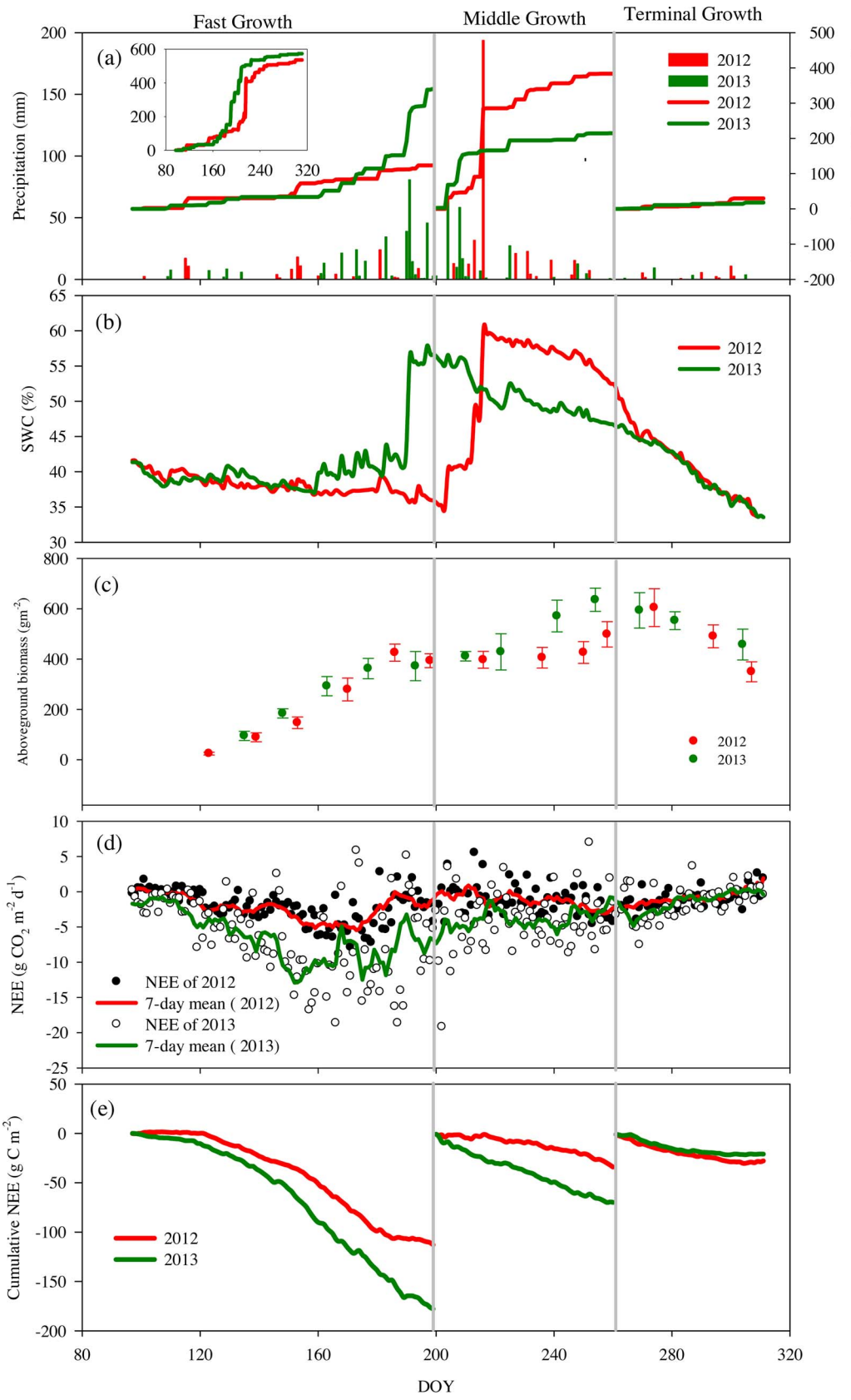

Fig. 2. Seasonal variations of (a) precipitation and cumulative precipitation of each growing periods (red line represents 2012, green line represents 2013), and the inset is the cumulative values of the entire growing seasons, (b) soil water content at 10 cm depth (SWC), (c) aboveground biomass, (d) daily integrated NEE, and (e) cumulative NEE of each growing periods of 2012 and 2013. (For interpretation of the references to colour in this figure legend, the reader is referred to the web version of this article.)

rainfall (Fig. 2a) and higher SWC (Fig. 2b, Table 1). At the beginning of the fast growth stage, because the biomass in the wetland was small (Fig. 2c), though with higher PAR and T_{air} (Table 1), the biomass development was still inhibited (Fig. 2c) due to the less precipitation in 2012 compared with that in 2013. As a result, the mean daily NEE values in 2012 (-2.2 ± 0.2 g CO_2 $m^{-2}day^{-1}$) was significantly lower than that in 2013 (-6.3 ± 0.5 g CO_2 $m^{-2}day^{-1}$) during the fast growth stage ($P < 0.01$). There was a parent increase in precipitation

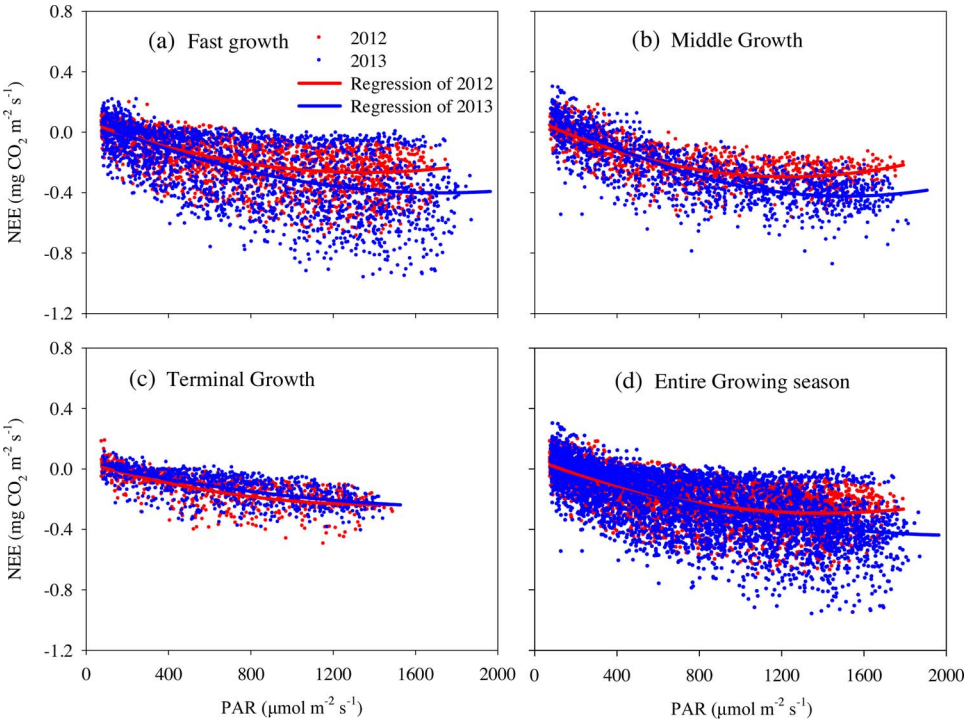

Fig. 3. Comparison of the light-response curves for net ecosystem CO_2 exchange (NEE) during growing seasons of 2012 and 2013. (a) the fast growth period, (b) the middle growth period, (c) the terminal growth period, and (d) the entire growing season. The curves were fitted using a rectangular hyperbola equation (equation (1)), and regression coefficients are presented in Table 2.

in 2012 compared with 2013 during the middle growth stage. However, higher SWC caused by higher precipitation did not augment the CO_2 uptake of 2012 but inhibited the CO_2 absorption, suggesting that plants may have experienced waterlogged stress. The mean daily NEE values during the middle growth stage in 2012 was -1.1 g CO_2 $m^{-2}day^{-1}$, which was distinctly lower than that in 2013 (-4.2 g CO_2 $m^{-2}day^{-1}$) ($P < 0.01$). During the terminal growth stage, there was no significant difference in mean daily NEE values between two yeas ($P > 0.05$). The dormancy of vegetation in the flux footprint area had a direct effect on NEE, with daily NEE values showing a rapid decrease and approaching zero during this growth stage. The cumulative NEE values were -112.8 and -177.7 g C m^{-2} during the fast growth stage, -34.1 and -69.8 g C m^{-2} during the middle growth stage, and -27.8 and -21.0 g C m^{-2} during the terminal growth stage, respectively (Fig. 2d and Table 1).

3.3. Responses of daytime NEE to light

The seasonal variations of parameters (A_{max}, α and $R_{eco,daytime}$) can be represented as single peak curves and be described by quadratic models (Fig. 3 and Table 2). During the fast growth stage, A_{max} and α in 2013 (0.84 mg CO_2 m^{-2} s^{-1} and 0.0024 mg CO_2 μmol^{-1}) were both significantly higher than those in 2012 (0.60 mg CO_2 m^{-2} s^{-1} and 0.0013 mg CO_2 μmol^{-1}) ($P < 0.01$). $R_{eco,day}$ in 2012 (0.12 mg CO_2 m^{-2} s^{-1}) was slightly higher than that in 2013 (0.09 mg CO_2 m^{-2} s^{-1}). Though it makes no differences in terms of α values in the two years during the middle growth stage, A_{max} and $R_{eco,day}$ in 2013 (0.87 mg CO_2 m^{-2} s^{-1} and 0.23 mg CO_2 m^{-2} s^{-1}) were significant higher than those in 2012 (0.60 mg CO_2 m^{-2} s^{-1} and 0.19 mg CO_2 m^{-2} s^{-1}) ($P < 0.01$). Though the vegetation senesced during the terminal growth stage, A_{max} in 2013 (0.65 mg CO_2 m^{-2} s^{-1}) was still significantly higher than that in 2012 (0.48 mg CO_2 m^{-2} s^{-1}) ($P < 0.01$), and $R_{eco,day}$ in 2013 (0.03 mg CO_2 m^{-2} s^{-1}) was lower than that in 2012 (0.07 mg CO_2 m^{-2} s^{-1}). Whereas A_{max} in 2013 (0.90 mg CO_2 m^{-2} s^{-1}) was significantly higher than that in 2012 (0.58 mg CO_2 m^{-2} s^{-1}), $R_{eco,day}$ in 2013 (0.09 mg CO_2 m^{-2} s^{-1}) was lower than that in 2012 (0.12 mg CO_2 m^{-2} s^{-1}), no differences were observed in α values throughout the entire growing season. Compared to 2012, much greater net carbon uptake was observed at the same PAR in 2013, which indicated that photosynthesis in 2013 was much higher than respiration.

3.4. Responses of nighttime NEE ($R_{eco,night}$) to air temperature and R_{eco} to gross primary production (GPP)

$R_{eco,night}$ was positively related to air temperature and can be expressed by the exponential function of the two years (Fig. 4) ($P < 0.01$). The temperature sensitivity of ecosystem respiration (Q_{10}) in 2012 (2.61) was slightly higher than that in 2013 (2.51) during the fast growth stage, and Q_{10} in 2012 (2.62) was higher than that in 2013

Table 2
Comparison of coefficients A_{max}, α and $R_{eco,day}$ estimated using equation (1) during each growing stages of 2012 and 2013 in the coastal wetland.

Growing period	A_{max} (mg CO_2 m^{-2} s^{-1})		α (mg CO_2 μmol^{-1})		$R_{eco,day}$ (mg CO_2 m^{-2} s^{-1})		R^2	
	2012	2013	2012	2013	2012	2013	2012	2013
Fast Growth (DOY 97–199)	0.60 ± 0.02	0.84 ± 0.05	0.0013 ± 0.0001	0.0024 ± 0.0001	0.12 ± 0.02	0.09 ± 0.02	0.41	0.37
Middle Growth (DOY 200–260)	0.60 ± 0.02	0.87 ± 0.02	0.0020 ± 0.0001	0.0021 ± 0.0001	0.19 ± 0.03	0.23 ± 0.03	0.59	0.64
Terminal Growth (DOY 261–311)	0.48 ± 0.04	0.65 ± 0.15	0.0013 ± 0.0001	0.0012 ± 0.0001	0.07 ± 0.02	0.03 ± 0.01	0.50	0.45
Entire growing season	0.58 ± 0.01	0.90 ± 0.04	0.0013 ± 0.0001	0.0014 ± 0.0001	0.12 ± 0.01	0.09 ± 0.01	0.46	0.43

Parameter α is the ecosystem apparent quantum yield, A_{max} is the ecosystem light-saturated net CO_2 exchange, $R_{eco,day}$ is ecosystem respiration in the daytime estimated from the NEE-PAR response curve, and R^2 is the coefficient of determination. Values of coefficients represent the mean ± SE.

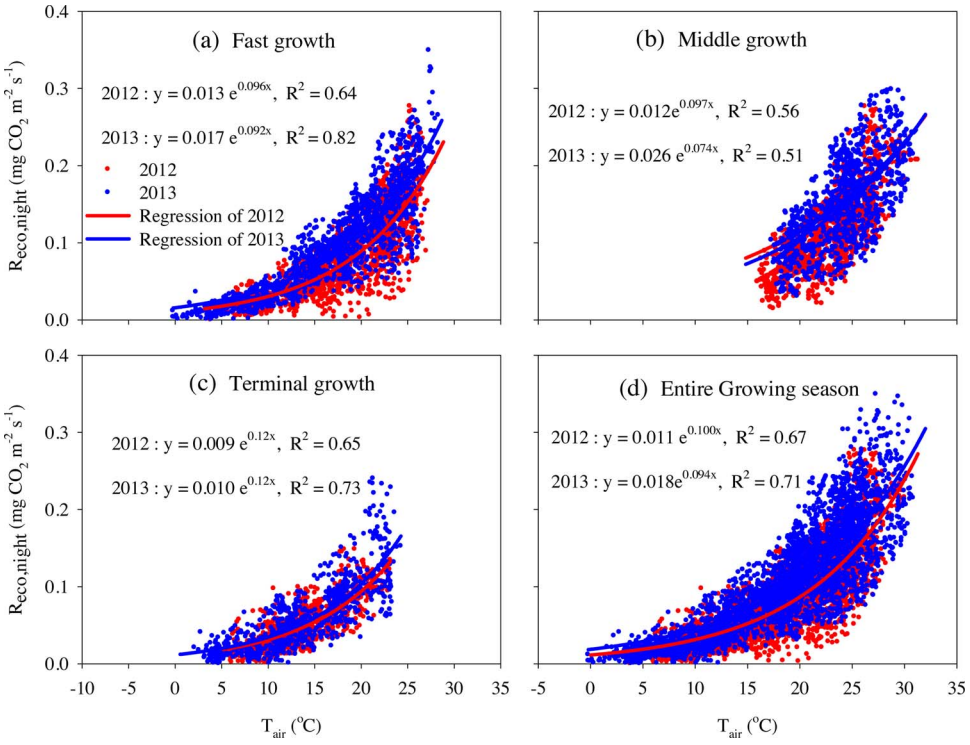

Fig. 4. Comparison of the temperature-response curves for nighttime NEE ($R_{eco,night}$) during growing seasons of 2012 and 2013. (a) the fast growth period, (b) the middle growth period, (c) the terminal growth period, and (d) the entire growing season. The curves were fitted with Eq. (2) based on the observed data.

(2.09) during the middle growth stage. Though the vegetation senesced during the terminal growth stage, the Q_{10} in 2012 (3.32) was higher than that in 2013 (3.18). For the entire growing season, the Q_{10} of R_{eco} was estimated to be 2.76 in 2012 and 2.56 in 2013, and a comparison of Q_{10} in the two years suggested that wetland in 2012 was more sensitive to changes in the air temperature than that in 2013.

Both years showed strong positive correlations of R_{eco} with GPP during each growing stages (Fig. 5). The data points of GPP plotted versus R_{eco} fell below/above the 1:1 line, indicating that GPP exceeded/belowed R_{eco} and the ecosystem was acting as a net C sink/source. The slope of line in 2012 was generally lower than that in 2013 during the growing stages except the terminal growth stage, indicating the weaker CO_2 absorption.

3.5. *Effect of changes of precipitation amount on the net photosynthetic rate during the different growth stages*

In the fast growth stage, precipitation under the +40% treatment significantly increased SWC (Fig. 6a), decreased soil salinity (Fig. 6c), and accelerated the net photosynthetic rate (Fig. 6e) compared to CK and −40% treatments ($P < 0.01$). SWC under the +40% treatment was 49.2%, which was 29% and 64% higher than the CK and −40% treatments ($P < 0.01$). Soil salinity under the +40% treatment was 5.1 ds m^{-2}, which was 9% and 26% lower than the CK and −40% treatments ($P < 0.01$). In addition, net photosynthetic rate under the +40% treatment was 15% and 25% higher than the CK and −40% treatments, respectively ($P < 0.01$). During the middle growth stage, though there were no significant differences of SWC and soil salinity ($P > 0.05$), net photosynthetic rate (Pn) under the −40% treatment was 45% and 69% higher than the CK and −40% treatments, respectively ($P < 0.01$).

4. Discussion

4.1. *Effect of the precipitation distribution on response of daytime NEE to light*

The precipitation distribution regulates the relationship between NEE and PAR response during the entire growing season. During the fast growth stage, driven by strong evaporation, water-soluble salts from the groundwater are transported upward to the root zone and soil surface through capillary rise (Zhang et al., 2011; Yao and Yang, 2013). Compared with 2012, higher NEE at the same PAR of 2013 (Fig. 3a) occurred due to an increased precipitation distribution (Fig. 2a) and lower salt stress, illustrating that increases in photosynthesis were much more than offset by increases in respiration during the fast growth stage. Studies have indicated that elevated salinity reduces annual gross ecosystem production (Heinsch et al., 2004), with most of the significant effects occurring during the first half of the growing season (Neubauer, 2013). The soil salinity concentration inhibits plant blade stomatal conductance and mesophyll conductance, causing the photosynthesis to decrease (Pezeshki and Patrick, 1987; Pezeshki et al., 2006), which decreases the growth rates of plants. The shift of precipitation to spring/summer (April-July) has the highest potential to change the productivity and composition of an ecosystem (Bates et al., 2006). Field and laboratory studies have suggested that the biomass and growth rates of many wetland plants decline as salinities increase (Mckee and Mendelssohn, 1989; Greiner et al., 2001; Krauss et al., 2009). The marsh on the Texas Gulf Coast was a net CO_2 sink during stages of high water availability and low sediment salinity and a net source when the water availability was low and salinity was high (Heinsch et al., 2004).

The wetland completely entered a monsoon both years during the middle growth stage, and episodic flooding was observed when the sediment beneath plants was near saturation prior to a heavy rainfall event. Our results showed that the waterlogged stress induced by flooding reduced both the maximum and net photosynthetic rate (Table 2, Fig. 6e), and subsequently reduced the daytime net CO_2 uptake during the middle growth stage. On the one hand, a monsoon

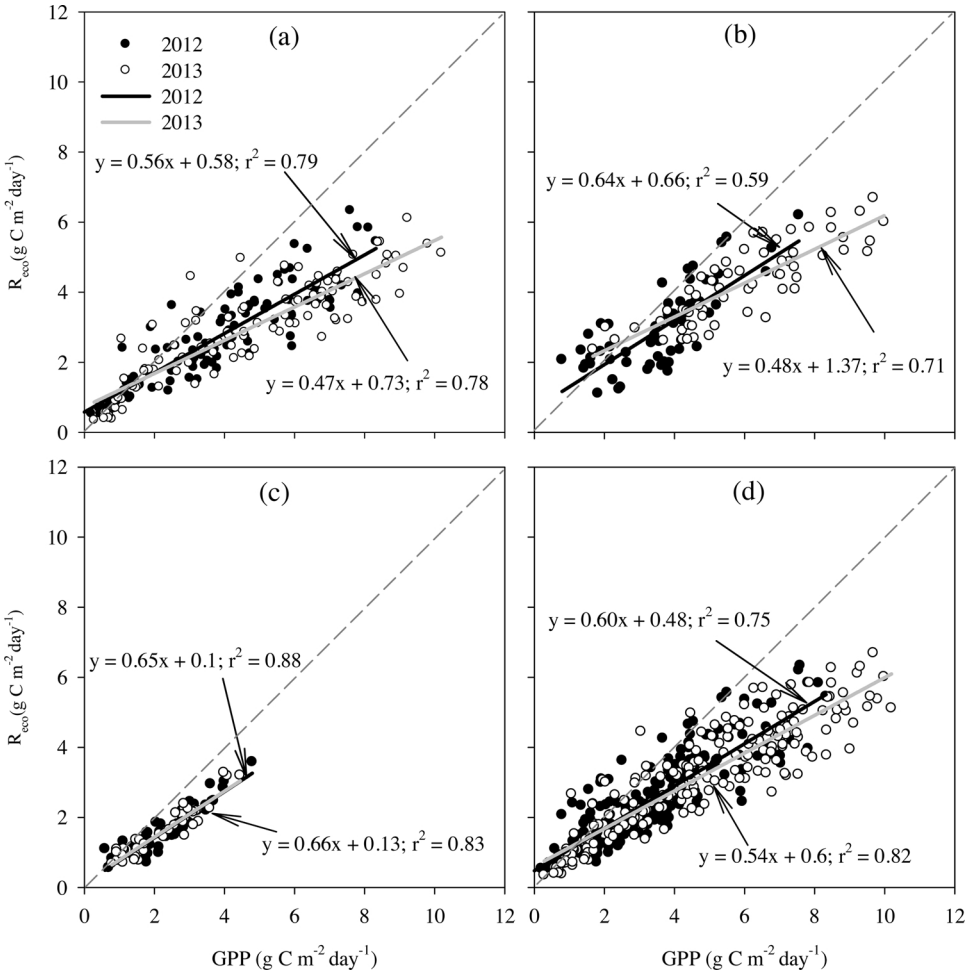

Fig. 5. Linear relationship between the daily values of ecosystem respiration (Reco) and gross primary production (GPP). (a) the fast growth period, (b) the middle growth period, (c) the terminal growth period, and (d) the entire growing season. Solid lines represent the regression line and dashed lines represent the 1:1 line. Rainy days were excluded from the analysis.

influences the relationship between solar and net radiation by depressing incoming solar radiation due to increased cloudiness and increasing net radiation due to decreased longwave radiation cooling and decreased albedo (Kwon et al., 2008). On the other hand, when wetlands are inundated, standing water and water in pores restrict the gas exchange between sediments and the atmosphere, and the effective photosynthetic leaf area may be reduced as some plant leaves are submerged (Schedlbauer et al., 2010; Jimenez et al., 2012) decreasing the maximum rates of photosynthesis. Meanwhile, flooding causes displacement of gases when soil pores are filled with water, and soil hypoxia or anoxia can decrease overall plant metabolic activity and force stomatal closure and transpiration cessation, which affect plant photosynthesis and autotrophic respiration (Banach et al., 2009; Dušek et al., 2009; Moffett et al., 2010; Schedlbauer et al., 2010). However, there was no significant difference between both years in terms of the NEE-PAR response curve during the terminal growth stage due to the vegetation senescing and the paucity of precipitation.

4.2. Effect of the precipitation distribution on response of $R_{eco,night}$ to air temperature

In our study, air temperature accounted for 67% and 71% of the variation in R_{eco} during the entire growing seasons of 2012 and 2013 (Fig. 4d), respectively, which was similar to those conducted in other wetland ecosystems (Lafleur et al., 2005; Zhou et al., 2009). In response to the limited precipitation, soil moisture gradually declined (Fig. 6a) during the fast growth stage, which coincided with the increase of soil salinity (Fig. 6c). Compared with 2013, lower $R_{eco,night}$ at the same temperature of 2012 (Fig. 4) was observed probably due to lower precipitation and higher salt stress during this stage. In contrast, the increase of soil salinity can cause plant cells to lose their water in response to osmotic stress, decreasing photosynthesis and primary productivity, which, in return, restrains aboveground respiration. Plant growth and maintenance respiration rates are tightly linked with photosynthetic activity (Cannell and Thornley, 2000), so the decline in ecosystem respiration of 2012 can be partially explained by salinity-related decreases in GPP due to the lower net photosynthetic rate (Figs. 5, 6 e). On the other hand, the increase of soil salinity can suppress microbial activity and decomposition rates of soil organic matter due to osmotic stress, leading to a decrease in sediment respiration (Chivers et al., 2010; Setia et al., 2010; Jimenez et al., 2012).

During the middle growth stage, though the inflow of freshwater after heavy rains tends to dilute the salinity in the wetland, waterlogged stress seemed more serious. Aboveground respiration was probably dominant for plants. Because the shoots and leaves were partially or completely submerged, water forms a diffusion barrier that restricts gas exchange, which would decrease overall plant metabolic activity such as photosynthesis and respiration (Banach et al., 2009). Studies have found that ecosystem respiration fell in parallel with gross photosynthesis, suggesting that a limited supply of photosynthetic substrates under waterlogged stress can suppress R_{eco} (Hussain et al., 2011). Sediment respiration probably included both aerobic and anaerobic processes. A low diffusion rate of oxygen in water results in limited oxygen availability for plant roots (Han et al., 2015). As a consequence, hypoxia or anoxia conditions lead to a switch of aerobic metabolism of plants into less efficient anaerobic fermentation, which can have a negative impact on Reco (Bailey-Serres and Voesenek, 2008; Sairam et al., 2008). As a result, ecosystem respiration was suppressed more in

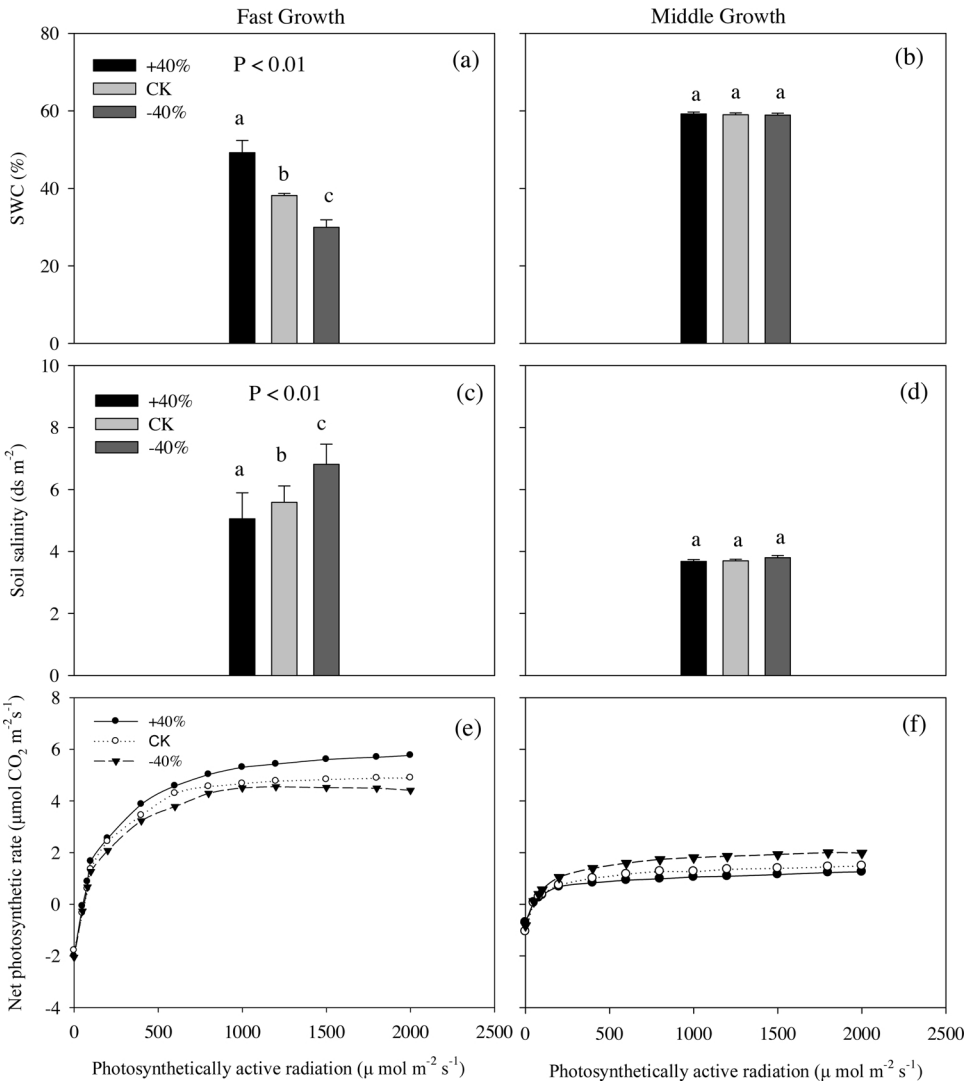

Fig. 6. Effect of changes in precipitation amount on soil water content at 10 cm depth (SWC) (a, b), soil salinity (c, d) at 10 cm depth, and Net photosynthetic rate (e, f) during the fast and middle growth periods. Different letters (a, b, c) indicate significant differences among different treatments. Bars represent means ± SE. +40%: precipitation increased by 40%; CK: no processing; −40%: precipitation reduced by 40%.

2012. Similar to the NEE−PAR response curve during the terminal growth stage (DOY 261–311), the R_{eco}-temperature curve between two years were slightly different but not significant. Due to the difference in the precipitation distribution throughout the entire growing season, R_{eco} in 2012 arguably suffered more salt stress (the early growth) and waterlogged stress (the middle growth) compared with 2013.

4.3. Effect of the precipitation distribution on carbon budget

On the growing season scale, the coastal wetland in the two years functioned as C sinks of -175 and -269 g C m^{-2}, respectively. An annual CO_2 balance of -164 g C m^{-2} was observed in 2012, and a higher net sink of -247 g C m^{-2} was estimated for 2013, which means the precipitation distribution during the growing season substantially affects the annual ecosystem CO_2 budget. Previous studies have suggested that droughts or wetness caused by the precipitation distribution in wetlands could affect NEE (Aurela et al., 2007; Hao et al., 2011; Lund et al., 2012), which coincided with the results in this study. Similar studies have also been conducted in temperate grassland (Hussain et al., 2011), semi-arid shrubland (Jia et al., 2016), subalpine meadows (Sloat et al., 2015), semi-arid pasture (Rajan et al., 2013) and forest ecosystems (Kljun et al., 2004; Bonal et al., 2008).

Our results demonstrated that the precipitation distribution in the growing season was critical to the sink/source strength. As the primary driver controlling NEE, precipitation could directly and indirectly affect the uptake of CO_2 during the growing season. During the fast growth stage, the inflow of freshwater after precipitation tends to dilute the salinity in the coastal wetland, which may accelerate net photosynthesis rate and promote plant growth (Fig. 2c), and consequently increase net CO_2 uptake (Table 1, Figs. 2 e, 5 a). During the middle growth stage, waterlogged stress induced by high precipitation could suppress net photosynthetic rate due to the partial or complete submersion of plants, as a result, the net CO_2 uptake was inhibited (Table 1, Figs. 2 e, 5 b). The same results have been found in a precipitation manipulation experiment in the same site (Fig. 6). Increased precipitation during the fast growth stage enhanced net photosynthetic rate (Fig. 6e) due to the reduced salt stress (Fig. 6c), whereas increased precipitation during the middle growth stage suppressed net photosynthetic rate (Fig. 6f) due to the increased waterlogged stress. Therefore, it is critical to take the precipitation distribution into account in forecasting the carbon budgets of coastal wetlands under global climate change.

4.4. Limitation of the research and outlook

The precipitation redistribution can affect the growth rate of plants, and vegetation structural characteristics are important for the seasonal ecosystem CO_2 exchange, but the leaf area index as an important biological process regulating CO_2 flux was not involved in our study. Moreover, the concentration of salt, groundwater and surface water depth were not measured during the observation stage. Our conclusion

are preliminary and further study involving longer time series spanning a wider range of precipitation conditions, biotic factors, salt and wetland hydrology are needed to confirm or refine these patterns, which is important for accurately evaluating the carbon budget and its controlling mechanisms over coastal wetlands.

5. Conclusion

This study provides a dual effect of precipitation redistribution on ecosystem CO_2 exchange in the coastal wetland. The higher precipitation promoted net ecosystem CO_2 absorption due to the increased SWC and reduced salt stress during the fast growth stage. While the higher precipitation suppressed net ecosystem CO_2 uptake due to the increased waterlogged stress during the middle growth stage. These results illustrated that the precipitation distribution could modify the magnitude of NEE as well as its response to light and temperature in coastal wetlands. Therefore, understanding the responses of NEE to the precipitation redistribution is essential not only for predictive modeling of potential short- and long-term changes of carbon storage but also for predicting the possible impacts of climate change

Acknowledgements

This work was founded by the National Nature Science Foundation of China (41671089) and the Science and Technology Service Network Initiative (KFJ-EW-STS-127). We also thank Liqiong Yang, Min Zhu, Bo Guan, Baohua Xie and two anonymous reviewers of their expert advice and fruitful comments.

References

Allen, M.R., Ingram, W.J., 2002. Constraints on future changes in climate and the hydrologic cycle. Nature 419, 224–232.
Aubinet, M., Grelle, A., Ibrom, A., Rannik, Ü., Moncrieff, J., Foken, T., Kowalski, A.S., Martin, P.H., Berbigier, P., Bernhofer, C., 1999. Estimates of the annual net carbon and water exchange of forests: the EUROFLUX methodology. Adv. Ecol. Res. 30, 113–175.
Aurela, M., Riutta, T., Laurila, T., Tuovinen, J.P., Vesala, T., Tuittila, E.S., Rinne, J., Haapanala, S., Laine, J., 2007. CO_2 exchange of a sedge fen in southern Finland – the impact of a drought period. Tellus B 59, 826–837.
Bailey-Serres, J., Voesenek, L.A.C.J., 2008. Flooding Stress: acclimations and genetic diversity. Annu. Rev. Plant Biol. 59, 313–339.
Baldocchi, D., Falge, E., Gu, L., Olson, R., Hollinger, D., Running, S., Anthoni, P., Bernhofer, C., Davis, K., Evans, R., 2001. FLUXNET: A new tool to study the temporal and spatial variability of ecosystem-scale carbon dioxide, water vapor, and energy flux densities. Bull. Am. Meteorol. Soc. 82, 2415–2434.
Baldocchi, D., 2008. 'Breathing'of the terrestrial biosphere: lessons learned from a global network of carbon dioxide flux measurement systems. Aust. J. Bot. 56, 1–26.
Banach, K., Banach, A.M., Lamers, L.P.M., Kroon, H.D., Bennicelli, R.P., Smits, A.J.M., Visser, E.J.W., 2009. Differences in flooding tolerance between species from two wetland habitats with contrasting hydrology: implications for vegetation development in future floodwater retention areas. Ann. Bot–London 103, 341–351.
Bates, J.D., Svejcar, T., Miller, R.F., Angell, R.A., 2006. The effects of precipitation timing on sagebrush steppe vegetation. J. Arid Environ. 64, 670–697.
Biederman, J.A., Scott, R.L., Goulden, M.L., Vargas, R., Litvak, M.E., Kolb, T.E., Yepez, E.A., Oechel, W.C., Blanken, P.D., Bell, T.W., 2016. Terrestrial carbon balance in a drier world: the effects of water availability in southwestern North America. Global Change Biol. 22, 1867–1879.
Bonal, D., Bosc, A., Ponton, S., Goret, J.Y., Burban, B., Gross, P., Bonnefond, J.M., Elbers, J., Longdoz, B., Epron, D., 2008. Impact of severe dry season on net ecosystem exchange in the neotropical rainforest of French Guiana. Global Change Biol. 14, 1917–1933.
Bowling, D.R., Bethers-Marchetti, S., Lunch, C.K., Grote, E.E., Belnap, J., 2015. Carbon, water, and energy fluxes in a semiarid cold desert grassland during and following multiyear drought. J. Geophys. Res.–Biogeosci. 115, 2393–2401.
Cannell, M., Thornley, J., 2000. Modeling the components of plant respiration: some guiding principles. Ann. Bot–London 85, 45–54.
Chivers, M.R., Turetsky, M.R., Waddington, J.M., Harden, J.W., Mcguire, A.D., 2010. Effects of experimental water table and temperature manipulations on ecosystem CO_2 fluxes in an alaskan rich fen. Ecosystems 12, 1329–1342.
Crooks, S., Herr, D., Tamelander, J., Laffoley, D., Vandever, J., 2011. Mitigating Climate Change Through Restoration and Management of Coastal Wetlands and Near-shore Marine Ecosystems: Challenges and Opportunities. Environment Department Paper 121. World Bank, Washington, DC.
Doughty, C., Metcalfe, D., Girardin, C., Malhi, Y., 2013. Impact of the 2010 drought on Amazonian carbon dynamics and fluxes. AGU Fall M.
Doughty, C.E., Metcalfe, D.B., Girardin, C.A.J., Amézquita, F.F., Cabrera, D.G., Huasco, W.H., Silva-Espejo, J.E., Araujo-Murakami, A., Costa, M.C.D., Rocha, W., 2015. Drought impact on forest carbon dynamics and fluxes in Amazonia. Nature 519, 78–82.
Drake, K., Halifax, H., Adamowicz, S.C., Craft, C., 2015. Carbon sequestration in tidal salt marshes of the northeast United States. Environ. Manage. 56, 998–1008.
Dušek, J., Čížková, H., Czerný, R., Taufarová, K., Šmídová, M., Janouš, D., 2009. Influence of summer flood on the net ecosystem exchange of CO_2 in a temperate sedge-grass marsh. Agric. For. Meteorol. 149, 1524–1530.
Easterling, D.R., Meehl, G.A., Parmesan, C., Changnon, S.A., Karl, T.R., Mearns, L.O., 2000. Climate extremes: observations, modeling, and impacts. Science 289, 2068–2074.
Falge, E., Baldocchi, D., Olson, R., Anthoni, P., Aubinet, M., Bernhofer, C., Burba, G., Ceulemans, R., Clement, R., Han, D., 2001. Gap filling strategies for defensible annual sums of net ecosystem exchange. Agric. For. Meteorol. 107, 43–69.
Fan, X., Pedroli, B., Liu, G., Liu, H., Song, C., Shu, L., 2011. Potential plant species distribution in the Yellow River Delta under the influence of groundwater level and soil salinity. Ecohydrology 4, 744–756.
Greiner, L.P.M.K., Grace, J.B., Hahn, E., Mendelssohn, I.A., 2001. The importance of competition in regulating plant species abundance along a salinity gradient. Ecology 82, 62–69.
Guan, Y.X., Liu, G.H., Wang, J.F., 2001. Saline-alkali land in the Yellow River Delta: amelioration zonation based on GIS. J. Geogr. Sci. 11, 313–320.
Han, G.X., Yang, L.Q., Yu, J.B., Wang, G.M., Mao, P.L., Gao, Y.J., 2013. Environmental controls on net ecosystem CO_2 exchange over a reed (Phragmites australis) wetland in the yellow river delta, China. Estuar. Coast. 36, 401–413.
Han, G.X., Chu, X.J., Xing, Q.H., Li, D.J., Yu, J.B., Luo, Y.Q., Wang, G.M., Mao, P.L., Rashad, R., 2015. Effects of episodic flooding on the net ecosystem CO_2 exchange of a supratidal wetland in the Yellow River Delta. J. Geophys. Res.–Biogeosci. 120, 1506–1520.
Hao, Y.B., Cui, X.Y., Wang, Y.F., Mei, X.R., Kang, X.M., Wu, N., Luo, P., Zhu, D., 2011. Predominance of precipitation and ttemperature controls on ecosystem CO_2 eexchange in zoige alpine wetlands of southwest China. Wetlands 31, 413–422.
Heinsch, F.A., Heilman, J.L., Mcinnes, K.J., Cobos, D.R., Zuberer, D.A., 2004. Carbon dioxide exchange in a high marsh on the Texas Gulf Coast: effects of freshwater availability. Agric. For. Meteorol. 125, 159–172.
Hussain, M.Z., Grünwald, T., Tenhunen, J.D., Li, Y.L., Mirzae, H., Bernhofer, C., Otieno, D., Dinh, N.Q., Schmidt, M., Wartinger, M., 2011. Summer drought influence on CO_2 and water fluxes of extensively managed grassland in Germany. Agr. Ecosyst. Environ. 141, 67–76.
IPCC, 2007. Climate Change 2007. The Physical Science Basis. Contribution of Working Group I to the Fourth Assesment Report of the Intergovernmental Panel on Climate Change. Cambridge University Press, Cambridge.
Iii, F.S.C., Woodwell, G.M., Randerson, J.T., Rastetter, E.B., Lovett, G.M., Baldocchi, D.D., Clark, D.A., Harmon, M.E., Schimel, D.S., Valentini, R., 2006. Reconciling carbon-cycle concepts, terminology, and methods. Ecosystems 9, 1041–1050.
Jia, X., Zha, T., Gong, J., Wang, B., Zhang, Y., Wu, B., Qin, S., Peltola, H., 2016. Carbon and water exchange over a temperate semi-arid shrubland during three years of contrasting precipitation and soil moisture patterns. Agric. For. Meteorol. 228, 120–129.
Jimenez, K.L., Starr, G., Staudhammer, C.L., Schedlbauer, J.L., Loescher, H.W., Malone, S.L., Oberbauer, S.F., 2012. Carbon dioxide exchange rates from short- and long-hydroperiod Everglades freshwater marsh. J. Geophys. Res.–Biogeosci. 117, 12751.
Kaimal, J.C., Finnigan, J.J., 1994. Atmospheric Boundary Layer Flows: Their Structure and Measurement. Oxford press, New York.
Kljun, N., Black, T.A., Gris, T.J., Barr, A.G., Gaumont-Guay, D., Morgenstern, K., Mccaughey, J.H., Nesic, Z., 2004. Net carbon exchange of three boreal forests during a drought. Agric. For. Meteorol. 23–27.
Knapp, A.K., Beier, C., Briske, D.D., Classen, A.T., Luo, Y., Reichstein, M., Smith, M.D., Smith, S.D., Bell, J.E., Fay, P.A., Heisler, J.L., Leavitt, S.W., Sherry, R., Smith, B., Weng, E., 2008. Consequences of more extreme precipitation regimes for terrestrial ecosystems. BioScience 58, 811–821.
Krauss, K.W., Doyle, T.W., Howard, R.J., 2009. Is there evidence of adaptation to tidal flooding in saplings of baldcypress subjected to different salinity regimes? Environ. Exp. Bot. 67, 118–126.
Kwon, H., Pendall, E., Ewers, B.E., Cleary, M., Naithani, K., 2008. Spring drought regulates summer net ecosystem CO_2 exchange in a sagebrush-steppe ecosystem. Agric. For. Meteorol. 148, 381–391.
Lafleur, P.M., Moore, T.R., Roulet, N.T., Frolking, S., 2005. Ecosystem respiration in a cool temperate bog depends on peat temperature but not water table. Ecosystems 8, 619–629.
Leppälä, M., Laine, A.M., Seväkivi, M.L., Tuittila, E.S., 2011. Differences in CO_2 dynamics between successional mire plant communities during wet and dry summers. J. Veg. Sci. 22, 357–366.
Liu, R., Cieraad, E., Li, Y., Ma, J., 2016. Precipitation pattern determines the inter-annual variation of herbaceous layer and carbon fluxes in a phreatophyte-dominated desert ecosystem. Ecosystems 601–614.
Lloyd, J., Taylor, J.A., 1994. On the temperature dependence of soil respiration. Funct. Ecol. 8, 315–323.
Lund, M., Christensen, T.R., Lindroth, A., Schubert, P., 2012. Effects of drought conditions on the carbon dioxide dynamics in a temperate peatland. Environ. Res. Lett. 7, 189–190.
Mckee, K.L., Mendelssohn, I.A., 1989. Response of a freshwater marsh plant community to increased salinity and increased water level. Aquat. Bot. 34, 301–316.
Min, Y., Liu, S., Yang, Z., Tao, S., Degloria, S.D., Holt, K., 2009. Effect on soil properties of conversion of Yellow River Delta ecosystems. Wetlands 29, 1014–1022.

Min, S.K., Zhang, X.B., Zwiers, F.W., Hegerl, G.C., 2011. Human contribution to more-intense precipitation extremes. Nature 470, 378–381.
Moffett, K.B., Adam, W., Berry, J.A., Gorelick, S.M., 2010. Salt marsh–atmosphere exchange of energy, water vapor, and carbon dioxide: effects of tidal flooding and biophysical controls. Water Resour. Res. 46, 5613–5618.
Nagy, Z., Pintér, K., Czóbel, S., Balogh, J., Horváth, L., Fóti, S., Barcza, Z., Weidinger, T., Csintalan, Z., Dinh, N.Q., 2007. The carbon budget of semi-arid grassland in a wet and a dry year in Hungary. Agric. Ecosyst. Environ. 121, 21–29.
Neubauer, S.C., 2013. Ecosystem responses of a tidal freshwater marsh experiencing saltwater intrusion and altered hydrology. Estuar. Coast. 36, 491–507.
Nie, M., Zhang, X.D., Wang, J.Q., Jiang, L.F., Yang, J., Quan, Z.X., Cui, X.H., Fang, C.M., Li, B., 2009. Rhizosphere effects on soil bacterial abundance and diversity in the Yellow River Deltaic ecosystem as influenced by petroleum contamination and soil salinization. Soil Biol. Biochem. 41, 2535–2542.
Noormets, A., Desai, A.R., Cook, B.D., 2008. Moisture sensitivity of ecosystem respiration Comparison of 14 forest ecosystems in the Upper Great Lakes Region, USA. Agric. For. Meteorol. 148, 216–230.
Pezeshki, S.R., Patrick, W.H., 1987. Effects of flooding and salinity on photosynthesis of Sagittaria lancifolia. Mar. Ecol. Program 41, 87–91.
Pezeshki, S.R., Laune Jr, R.D.D., W.H.P, 2006. Response of freshwater marsh species, Panicum hemitomen Schultz, to increased salinity. Freshwater Biol. 17, 195–200.
Polsenaere, P., Lamaud, E., Lafon, V., Bonnefond, J.M., Bretel, P., Delille, B., Deborde, J., Loustau, D., Abril, G., 2012. Spatial and temporal CO_2 exchanges measured by Eddy Covariance over a temperate intertidal flat and their relationships to net ecosystem production. Biogeosciences 9, 249–268.
Rajan, N., Maas, S.J., Song, C., 2013. Extreme drought effects on carbon dynamics of a semiarid pasture. Agron. J. 105, 1749–1760.
Ross, I., Misson, L., Rambal, S., Arneth, A., Scott, R.L., Carrara, A., Cescatti, A., Genesio, L., 2012. How do variations in the temporal distribution of rainfall events affect ecosystem fluxes in seasonally water-limited Northern Hemisphere shrublands and forests? Biogeosciences 9, 1007–1024.
Ruimy, A., Jarvis, P.G., Baldocchi, D.D., Saugier, B., 1995. CO_2 Fluxes over plant canopies and solar radiation. Rev. Adv. Ecol. Res. 26, 1–68.
Sairam, R.K., Kumutha, D., Ezhilmathi, K., Deshmukh, P.S., Srivastava, G.C., 2008. Physiology and biochemistry of waterlogging tolerance in plants. Biol. Plant. 52, 401–412.
Schedlbauer, J.L., Oberbauer, S.F., Starr, G., Jimenez, K.L., 2010. Seasonal differences in the CO_2 exchange of a short-hydroperiod Florida Everglades marsh. Agric. For. Meteorol. 150, 994–1006.
Scott, R.L., Biederman, J.A., Hamerlynck, E.P., Barron-Gafford, G.A., 2015. The carbon balance pivot point of southwestern U.S. semiarid ecosystems: insights from the 21 st century drought. J. Geophys. Res.–Biogeosci. 120, 2612–2624.
Semenov, V., Bengtsson, L., 2002. Secular trends in daily precipitation characteristics: greenhouse gas simulation with a coupled AOGCM. Clim. Dyn. 19, 123–140.
Setia, R., Marschner, P., Baldock, J., Chittleborough, D., 2010. Is CO_2 evolution in saline soils affected by an osmotic effect and calcium carbonate? Biol. Fertil. Soils 46, 781–792.
Sloat, L.L., Henderson, A.N., Lamanna, C., Enquist, B.J., 2015. The effect of the foresummer drought on carbon exchange in subalpine meadows. Ecosystems 18, 533–545.
Webb, E.K., Pearman, G.I., Leuning, R., 1980. Correction of flux measurements for density effects due to heat and water vapour transfer. Q. J. R. Meteorol. Soc. 106, 85–100.
Wu, Z., Dijkstra, P., Koch, G.W., Peñuelas, J., Hungate, B.A., 2011. Responses of terrestrial ecosystems to temperature and precipitation change: a meta-analysis of experimental manipulation. Global Change Biol. 17, 927–942.
Yao, R., Yang, J., 2013. Quantitative evaluation of soil salinity and its spatial distribution using electromagnetic induction method. Agric. Water Manage. 97, 1961–1970.
Zhang, T.T., Zeng, S.L., Gao, Y., Ouyang, Z.T., Li, B., Fang, C.M., Zhao, B., 2011. Assessing impact of land uses on land salinization in the Yellow River Delta, China using an integrated and spatial statistical model. Land Use Policy 28, 857–866.
Zhong, Q., Du, Q., Gong, J., Zhang, C., Wang, K., 2013. Effects of in situ experimental air warming on the soil respiration in a coastal salt marsh reclaimed for agriculture. Plant Soil. 371, 1–16.
Zhou, L., Zhou, G., Jia, Q., 2009. Annual cycle of CO_2 exchange over a reed (Phragmites australis) wetland in Northeast China. Aquat. Bot. 91, 91–98.